Research Article

A New Mechanical Model for Particle Transport by Surface Waves and Applications

Minvydas Ragulskis,[1] Edita Sakyte,[1] Jesús M. Seoane,[2] and Miguel A. F. Sanjuán[2]

[1] *Department of Mathematical Research in Systems, Kaunas University of Technology, Studentu 50-222, 51638 Kaunas, Lithuania*

[2] *Nonlinear Dynamics, Chaos and Complex Systems Group, Department of Physics, University Rey Juan Carlos, Tulipán s/n, 28933 Móstoles, Madrid, Spain*

Correspondence should be addressed to Miguel A. F. Sanjuán, miguel.sanjuan@urjc.es

We present a study of the behavior of a ball under the influence of gravity on a platform. A propagating surface wave travels on the surface of the platform while the platform remains motionless. This is a modification of the classical bouncing ball problem and describes the transport of particles by surface waves. Phase and velocity maps cannot be expressed in the explicit form due to implicit formulations, and no formal analytical analyses is possible. Numerical analysis shows that the transition to chaos is produced via a period doubling route which is a common property for classical bouncers. These numerical analysis have been carried out for the conservative and for the viscous cases and also for elastic and for inelastic collisions. The bouncing process can be sensitive to the initial conditions and can be useful for control techniques which can dramatically increase the effectiveness of particle transport in practical applications. Finally, we also consider the mechanical model of a particle sliding on a surface which is also important because it has important physical implications such as the transportation of thin films in biomedical applications, among others.

1. Introduction

A particle falling down, in a constant gravitational field, on a moving platform is called a bouncing ball problem, or a bouncer. This model was suggested more than thirty years ago [1, 2] as an alternative to the Fermi-Ulam model [3] of cosmic ray acceleration [4]. In the ensuing years many approaches to the bouncer model have been studied theoretically and experimentally [5–8]. It has been proved to be a useful system for experimentally exploring several new nonlinear effects [9, 10]. Moreover, it has been implemented into a number of engineering applications [11, 12].

The bouncer model can be briefly characterized by the following basic statements. (i) Maps derived for the bouncer model can be exactly iterated for any time function describing the moving platform [7, 9] (though usually the platform is assumed to oscillate with a single frequency). (ii) The ball-platform collisions can be characterized by a coefficient of restitution α changing from $\alpha = 1$ for a perfectly elastic case to $\alpha = 0$ for a completely inelastic situation. (iii) The chaotic bouncer can be easily used to relate theoretical predictions to experimental results, [9, 10] what makes it a paradigm model in nonlinear dynamics.

In this paper we assume that a particle is falling down in a constant gravitational field on a stationary platform. A propagating surface wave travels on the surface of the platform while the platform remains motionless. Such a model can be used to describe the transport of particles by propagating surface waves, which is an important problem with numerous applications. Powder transport by piezoelectrically excited ultrasonic surface waves [13], manipulation of bioparticles using traveling wave electrophoresis [14, 15], and conveyance of submerged buoys in coastal waters [16] are just a few examples of problems involving the interaction between propagating waves and transported bouncing particles.

This paper is organized as follows. In Section 2 we present a complete description of our model, the bouncer system. Section 3 presents numerical simulations showing that the modified bouncer model possesses such an inherent chaotic dynamics. These results are carried out for both, the conservative and the dissipative cases. The case of a particle sliding on the surface is fully analyzed in Section 4. Conclusions and discussions of the main results of this paper are presented in Section 5.

2. Model Description

We consider the two-dimensional system shown in Figure 1, where the surface of an elastic plate is represented by a solid line which coincides with the x-axis in the state of equilibrium. A point of the surface in the state of equilibrium $(x, 0)$ is translated to coordinates (X, Y) when a wave process takes place. This translation is sensitive to time t and coordinate x:

$$X = x + \eta(x, t),$$
$$Y = \zeta(x, t),$$

(2.1)

where the functions $\eta(x, t)$ and $\zeta(x, t)$ determine deflections from the state of equilibrium.

Explicitly, the longitudinal and transverse displacements of the medium at the surface of flat boundary with travelling Rayleigh wave can be expressed like [17]

$$u_x = \frac{\omega}{\chi}\sqrt{\frac{2\rho(1+v)}{E}}\left(1 - \frac{\sqrt{1-\chi^2}\sqrt{2(1-v)-\chi^2(1-2v)}}{(1-0.5\chi^2)\sqrt{2(1-v)}}\right)C\,\sin(\omega t \mp kx),$$

$$u_y = \frac{\omega}{\chi}\sqrt{\frac{2\rho(1+v)}{E}}\left(1 - \frac{\sqrt{2(1-v)-\chi^2(1-2v)}}{\sqrt{2(1-v)}}\right)0.5\chi^2 C\,\cos(\omega t \mp kx),$$

(2.2)
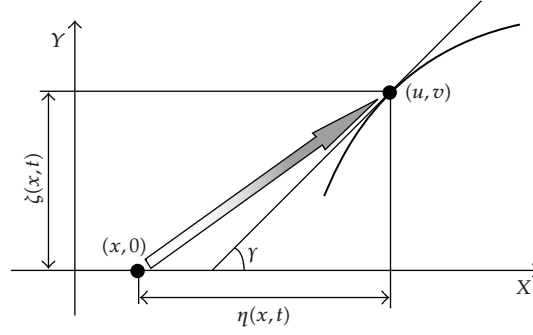
Figure 1: Schematic diagram illustrating the collision between the particle and the surface.

where u_x and u_y are the longitudinal and transverse displacements, x the coordinate of the surface point of the medium before the wave process took place; C is a constant, k the wavenumber and ρ the density. χ can be found from the following algebraic equation:

$$\chi^6 - 8\chi^4 + 8\left(3 - \frac{1-2\nu}{1-\nu}\right)\chi^2 - 16\left(1 - \frac{1-2\nu}{2(1-\nu)}\right) = 0, \tag{2.3}$$

and the angular velocity ω can be found from the following transcendental equation:

$$\left(k^2 + \beta^2\right)^2 \cosh(\alpha a)\sinh(\beta a) - 4k^2\alpha\beta\cosh(\beta a)\sinh(\alpha a) = 0, \tag{2.4}$$

where $\alpha = \sqrt{(v_l k^2 - \omega^2)/v_l^2}$, $\beta = \sqrt{(v_t k^2 - \omega^2)/v_t^2}$, $v_l = \sqrt{(\lambda + 2\mu)/\rho}$ and $v_t = \sqrt{\mu/\rho}$, ν the Poisson's ratio and λ the first Lamé constant. It can be noted that the ratio between the amplitudes of transverse and longitudinal deformations depends on ν. In usual elastic media it is quite normal that the transverse displacement is about 1.5 times larger than the longitudinal displacement [18]. The motion of a point in the medium is an ellipse. Also, the direction of the velocity of the particles at the peaks of the wave is opposite to the direction of wave propagation.

Rayleigh waves are dispersive due to a dependence of the wave's speed on its wavelength. Typical example is Rayleigh waves in the Earth where waves with a higher frequency travel more slowly than those with a lower frequency. Rayleigh waves thus often appear spread out on seismograms recorded at distant earthquake recording stations [19]. Surface acoustic waves (SAWs) generated by SAW devices on rough anisotropic materials also experience considerable dispersion [20]. On the other hand, film waves generated on a surface of a finite liquid bed [21] can be characterized by a single frequency wave component. Therefore we concentrate on a one single frequency steady-state Rayleigh wave propagation and disregard dispersion.

Whenever a traveling nondispersive Rayleigh surface wave occurs in a medium, it can be characterized by a retrograde elliptic motion of the particles of that medium:

$$\eta(x,t) = a\,\sin(\omega t - kx),$$
$$\zeta(x,t) = b\,\cos(\omega t - kx), \tag{2.5}$$

where a and b are longitudinal and transverse amplitudes of the oscillations; ω is the angular frequency, and k is the wave number. Remind that in a usual elastic medium it is quite normal for the transverse displacement to be about 1.5 times larger than the longitudinal displacement [18].

The coordinates of the particle are denoted as (u, v). Assume that the particle is in contact with the surface at time moment t, then the following constrain takes place:

$$v = \zeta(x, t),\tag{2.6}$$

where x is to be found from the following algebraic equality (where u and t are given and x is the unknown):

$$x + \eta(x, t) = u.\tag{2.7}$$

In other words, the instantaneous shape of the surface cannot be described by an explicit function. Nevertheless, the tangent to the surface at the point with abscise u can be expressed explicitly:

$$\tan \gamma = \frac{\partial \zeta(x, t)/\partial x}{1 + \partial \eta(x, t)/\partial x},\tag{2.8}$$

where γ is the angle between the tangent and the x-axis. Instantaneous velocities (x- and y-components) of the point of the surface in contact with the particle can be expressed as $\partial \eta(x, t)/\partial t$ and $\partial \zeta(x, t)/\partial t$ accordingly.

The governing equations of motion of a particle in a free flight mode are

$$m\ddot{u} + h\dot{u} = 0,$$
$$m\ddot{v} + h\dot{v} = -mg,\tag{2.9}$$

where top dots denote full derivative by time, m is the mass of the particle, h is the coefficient of viscous damping of the media above the surface, and g is the free fall acceleration. Initial conditions $u(t_0) = u_0; \dot{u}(t_0) = \dot{u}_0; v(t_0) = v_0; \dot{v}(t_0) = \dot{v}_0$ yield partial solutions:

$$u(t) = u_0 + \dot{u}_0 \frac{m}{h}\left(1 - \exp\left(-\frac{h}{m}(t - t_0)\right)\right);$$

$$\dot{u}(t) = \dot{u}_0 \exp\left(-\frac{h}{m}(t - t_0)\right);$$

$$v(t) = v_0 + \left(\dot{v}_0 + \frac{mg}{h}\right)\frac{m}{h}\left(1 - \exp\left(-\frac{h}{m}(t - t_0)\right)\right) - \frac{mg}{h}(t - t_0);\tag{2.10}$$

$$\dot{v}(t) = \dot{v}_0 \exp\left(-\frac{h}{m}(t - t_0)\right) - \frac{mg}{h}\left(1 - \exp\left(-\frac{h}{m}(t - t_0)\right)\right).$$

The free flight stage continues until the particle collides with the surface. Unfortunately, it is impossible to determine the explicit time moment of the collision due to the

fact that the instantaneous shape of the surface cannot be expressed by an explicit function. Instead, one has to use iterative numerical techniques in order to determine the exact moment of the bounce.

Localization of the root (the time moment of the collision) is performed using a time marching technique starting from the initial conditions until

$$v(t_0 + i \cdot \Delta t) < \zeta(x_i, t_0 + i \cdot \Delta t) \tag{2.11}$$

where Δt is the time step; $i = 1, 2, \ldots, r$; r is the step number for which (4.8) is satisfied for the first time, and x_i is the solution of (4.4) at fixed i:

$$x_i + \eta(x_i, t_0 + i \cdot \Delta t) = u(t_0 + i \cdot \Delta t); \tag{2.12}$$

and $u(t_0 + i \cdot \Delta t)$, $v(t_0 + i \cdot \Delta t)$ are determined by (4.7). Solution of (4.9) also requires an iterative numerical algorithm.

When the root $\hat{t}$ is localized in the interval $t_0 + (r - 1) \cdot \Delta t < \hat{t} \le t_0 + r \cdot \Delta t$, one needs to fine down the value of $\hat{t}$ using an iterative computational algorithm. This iterative algorithm can be a most simple bisection method, though more sophisticated algorithms comprising the golden section rule or Newton's iterations for example can be used instead until the desirable accuracy is achieved. As the collision moment $\hat{t}$ is fined down in every iteration, the coordinate $\hat{x}$ (corresponding to the collision point $\hat{u} : \hat{x} + \eta(\hat{x}, \hat{t}) = \hat{u}$) is also made more precise. Initially, $x_{r-1} < \hat{x} \le x_r$; every iteration helps to reach a better accuracy.

Such iterative method of determination of the collision moment leads us to the important conclusion that phase and velocity maps cannot be expressed in an explicit form, and no formal analytical analysis is possible.

Nevertheless, the geometrical coordinates of the point of collision are $(\hat{u}; \zeta(\hat{x}, \hat{t}))$ and can be reconstructed using computational techniques. Velocities of the particle just before the collision are $\dot{u}(\hat{t})$ and $\dot{v}(\hat{t})$. Similarly, instantaneous velocities of the surface in contact with the particle are $\eta'_t(\hat{x}, \hat{t})$ and $\zeta'_t(\hat{x}, \hat{t})$.

Projections of the particle's velocities just before the collision to the normal and to the tangent to the surface at the contact point can be expressed in the following form:

$$\hat{P}_n = -\dot{u}(\hat{t}) \sin \gamma + \dot{v}(\hat{t}) \cos \gamma,$$
$$\hat{P}_t = \dot{u}(\hat{t}) \cos \gamma + \dot{v}(\hat{t}) \sin \gamma, \tag{2.13}$$

where the angle γ is determined from (4.5) at the point of collision.

Analogously, projections of velocities of the point of the surface in contact with the particle to the normal and to the tangent take the following form:

$$\dot{S}_n = -\eta'_t(\hat{x}, \hat{t}) \sin \gamma + \zeta'_t(\hat{x}, \hat{t}) \cos \gamma,$$
$$\dot{S}_t = \eta'_t(\hat{x}, \hat{t}) \cos \gamma + \zeta'_t(\hat{x}, \hat{t}) \sin \gamma. \tag{2.14}$$

Then, the velocities of the particle just after the collision (in the normal and tangent directions) are

$$
\dot{P}_n = (1 + \alpha)\dot{S}_n - \alpha\widehat{\dot{P}}_n,
$$
$$
\dot{P}_t = \beta\dot{S}_n - (1 + \beta)\widehat{\dot{P}}_t,
$$

(2.15)

where α is the coefficient of restitution for the collision in the normal direction. This constant is a measure of the energy loss at each impact. For elastic collisions $\alpha = 1$, and $\alpha < 1$ for inelastic collisions. Coefficient β determines the friction between the particle and the surface at the moment of collision. There is no friction between the particle and the surface when $\beta = 0$. The utmost value $\beta = 1$ represents the situation when the projection of the particle's velocity (immediately after the impact) and the projection of the surface's point velocity to the tangent are equal.

The free flight stage starts over again immediately after the collision, and the initial conditions are

$$
u(\widehat{t}) = \widehat{u},
$$
$$
\dot{u}(\widehat{t}) = -\dot{P}_n \sin \gamma + \dot{P}_t \cos \gamma,
$$
$$
v(\widehat{t}) = \zeta(\widehat{x}, \widehat{t}),
$$
$$
\dot{v}(\widehat{t}) = \dot{P}_n \cos \gamma + \dot{P}_t \sin \gamma.
$$

(2.16)

The presented model is a modification of the classic bouncer model which can be derived assuming $\zeta(x, t) = b\cos(\omega t)$ and $\eta(x, t) = 0$. In that case $u = x$, and the model becomes explicit.

3. Complex Dynamics in the Modified Bouncer Model

We will demonstrate that the modified bouncer model possesses such an inherent feature as chaotic dynamics. Moreover, we will show that the sensitivity to initial conditions can be exploited for the control of the process of conveyance. We will show these results for the conservative or nonviscous case ($h = 0$) and for the viscous case ($h \neq 0$).

3.1. Nonviscous Case

We take $h = 0$, for which the media above the surface is non-viscous, $\alpha = 1$ (elastic collisions) and $\beta = 0$ (no damping generated by sliding).

The dynamics of a bouncing particle on a surface of a propagating wave is very sensitive to the initial conditions if the dynamics is Hamiltonian. Apparently, it is possible to find such a set of initial conditions which lead to regular and periodic dynamics. This is illustrated in Figure 2 where collision heights $v(\widehat{t})$ are plotted versus initial velocity $\dot{u}(0)$. 50 successive collisions are used for every discrete value of $\dot{u}(0)$ to produce this diagram. The
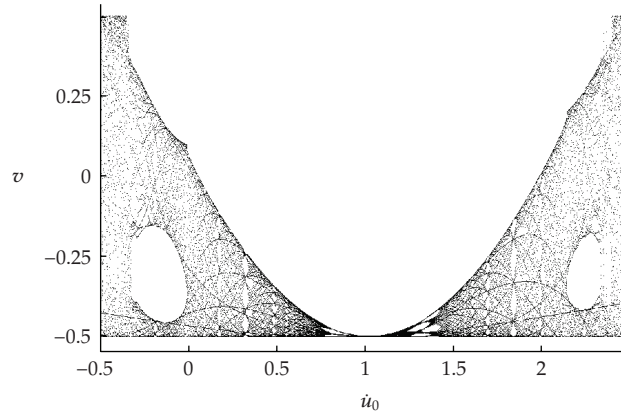
Figure 2: Collision heights $v(\hat{t})$ plotted versus initial velocity $\dot{u}(0)$ for $\dot{u}(0) = \omega/k$ at $\omega = 1$, $k = 1$, $m = 0.5$, $g = 1$, $a = b/1.5$, $u(0) = \pi$, $v(0) = 0$, and $\dot{v}(0) = -0.5$.
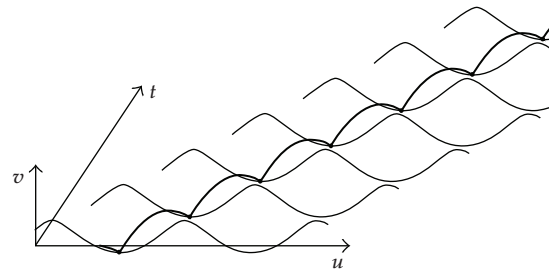
Figure 3: Period 1 trajectory of a bouncing particle for $\omega = 1$, $k = 1$, $m = 0.5$, $g = 1$, $a = b/1.5$, $u(0) = \pi$, $\dot{u}(0) = 1$, $v(0) = 0$, and $\dot{v}(0) = -0.5$.
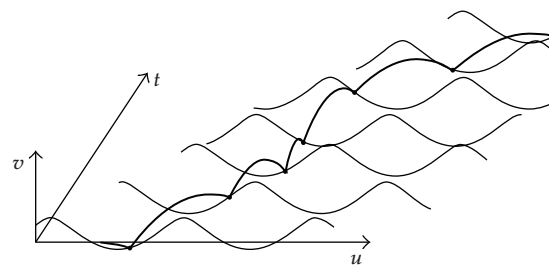
Figure 4: Chaotic trajectory of a bouncing particle for $\omega = 1$, $k = 1$, $m = 0.5$, $g = 1$, $a = b/1.5$, $u(0) = \pi$, $\dot{u}(0) = 2$, $v(0) = 0$, and $\dot{v}(0) = -0.5$.

initial condition $\dot{u}(0) = \omega/k$ produces a period 1 motion at $\omega = 1$, $k = 1$, $m = 0.5$, $g = 1$, $a = b/1.5$, $u(0) = \pi$, $v(0) = 0$ and, $\dot{u}(0) = -0.5$. This is illustrated in Figure 3.

We plot the trajectory of the particle in 3D for better visual interpretation. Collision moments are marked as black dots. At every moment of collision we also plot the instantaneous shape of the surface (one can note that the instantaneous shape of the surface is not harmonic). One can clearly see the difference in the complexity of the particle dynamics at $\dot{u}(0) = 1$ (see Figure 3) and $\dot{u}(0) = 2$ (see Figure 4).

(a)

(b)
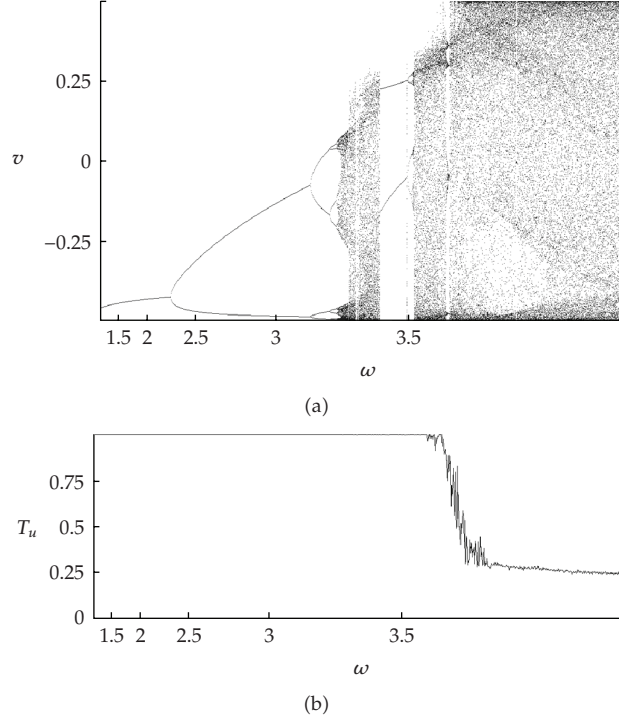
Figure 5: Transport of particles at increasing wave speeds (elastic collisions, viscous media over the surface). Reduced impact representation (a) shows the transition to chaos via a period doubling route. Note that impact heights are distributed in the interval $[-0.5, 0.5]$. Nondimensional longitudinal particle's transport velocity T_u drops down at higher wave speeds due to the viscosity of the media above the surface (b). System's parameters are $\alpha = 1$; $\beta = 0$; $\eta(x, t) = (2/3) \sin(\omega t - x)$; $\zeta(x, t) = (1/2)\cos(\omega t - x)$; $h = 0.1$; $m = 0.5$; $g = 9.81$.

3.2. Viscous Case

For this case, we assume that collisions are completely elastic ($\alpha = 1$), and there is no tangential friction between the particle and the surface ($\beta = 0$), but the media above the surface is viscous fixing the value of $h = 0.1$ as in [22]. We use the reduced impact representation, where the height of the bouncing ball is sampled at each impact with the surface (impact sampling). Since the system is dissipative, we plot the bouncing process after the initial transients cease down (see Figure 5(a)). We skip 1500 successive bounces before starting to plot the collision heights $v(t)$ for every discrete value of ω. Parameter ω is varied following the rule $\omega_i = 1 + (3/\ln 21) \ln(1 + 20i/1024)$; $i = 1, \ldots, 1024$, which helps to expand the cascade of period doubling bifurcations. The control parameter in our case is not the amplitude of the platform's oscillation but the velocity of the wave propagation; the collision height is used instead of collision velocity for a reduced impact representation. Moreover, the media above the surface of the plate is viscous. It appears that the transition to chaos via a period doubling route observed for a classical bouncer [23] is observed also for a particle bouncing on a surface of a stationary platform with a propagating wave traveling on its surface.

A phenomenological model could be used to exemplify the bifurcation diagram presented in Figure 5(a). The logistic map [24] is probably the simplest model ever used to

study the transition to chaos via a period doubling route. Simple computational experiments with appropriately chosen parameter values of the logistic map would illustrate the universality of the bifurcation diagram in Figure 5(a).

An important parameter characterizing the effectiveness of the transport is the average longitudinal velocity of the particle $\bar{u}$. We average it over a long period of time after the initial transients cease down. In order to calculate a nondimensional quantity we divide it from the velocity of the traveling wave $T_u = k\bar{u}/\omega$. Thus, the average velocity of conveyance is equal to the velocity of the traveling wave if T_u is equal to 1 as shown in Figure 5(b).

It is interesting to observe that the particle is transported with the average velocity of the traveling wave until the period 3 bouncing mode after a cascade of period doubling bifurcations (see Figure 5(a)). The particle's average transportation velocity drops down only when the period 3 bouncing mode experiences its own cascade of period doubling bifurcations. External damping forces acting to the particle prevent its motion with the average wave's velocity in the direction of the wave propagation when this velocity becomes large enough (even though the collisions are elastic). Also, the bouncing process is insensitive to initial conditions–eventually it converges to the one and only attractor shown in Figure 5(a) (at fixed ω).

Figures 6(a)–6(d) show different dynamical behaviors of the transient processes for the elastic case ($\alpha = 1$) once we fixed the parameter values as follows: $\beta = 0$, $k = 1$, $m = 0.5$, $g = 9.81$, $b = 0.5$, and $a = b/1.5$. We obtain both, periodic and chaotic motions depending on the value of the parameter ω. Figures 6(a)–6(c) show for $\omega = 2$, $\omega = 3$, and $\omega = 3.45$ period 1, period 2, and period 3 processes, respectively. Chaotic bouncing for the value $\omega = 4$ is shown in Figure 6(d).

The situation becomes different when collisions are inelastic, as shown in [22]. In the presence of inelastic collisons, a vanishing bouncing process takes place (complete chattering [23]) when the particle sets into the state of rest on a slope of the propagating wave. The term *complete chattering* is used in literature to describe the process when the time interval between inelastic bounces tends to zero and the ball finally "sticks" to the surface of the oscillating platform. As we mentioned previously, a complete description of this phenomenon is given in [22].

4. The Sliding Particle Model

In this section we thoroughly analyze the case in which the particle is sliding on the surface instead of the case in which it is falling down on it, analyzed previously. Our motivation is the following. Conveyance of particles and bodies by propagating waves is an important scientific and engineering problem with numerous applications. Manipulation of bioparticles and gene expression profiling using traveling wave dielectrophoresis [14, 25, 26], segregation of particles in suspensions subject to ac electric fields [27], transport of sand particles and oil spills in coastal waters [28, 29], powder transport by piezoelectrically excited ultrasonic waves [13, 22], transportation of thin films in biomedical applications [21] are just a few examples of problems involving interaction between propagating waves and transported objects.

We now describe, as in the bouncer model, the equations of motions of our sliding particle model.

It is assumed that a mass particle is in contact with the deformed surface at a point (u, v) at a time moment t (Figure 7). A point of the surface in the equilibrium state $(x, 0)$ is

(a)

(b)

(c)

(d)
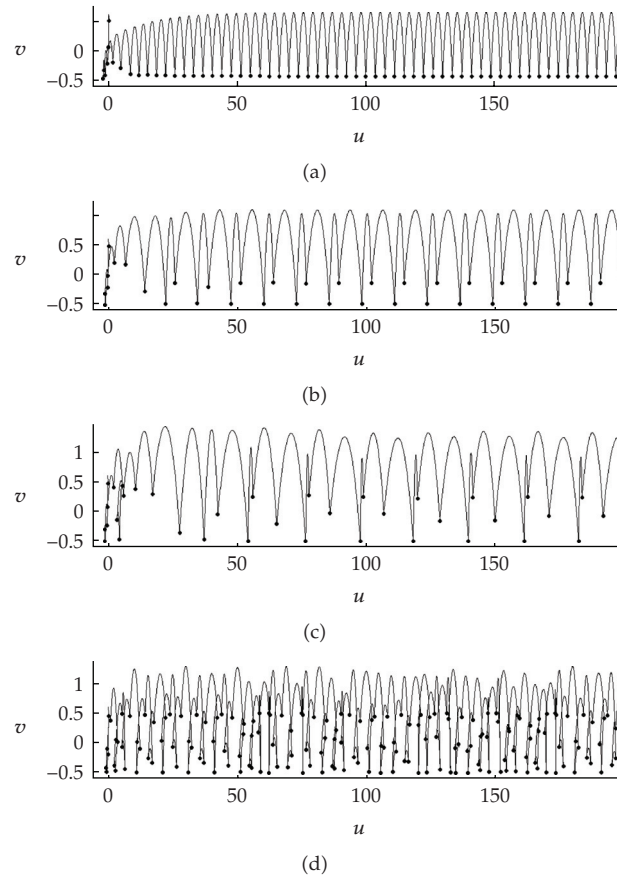
Figure 6: Transient processes for parameter values as follows: $h = 0.1$, $\alpha = 1$, $\beta = 0$, $k = 1$, $m = 0.5$, $g = 9.81$, $b = 0.5$, and $a = b/1.5$. We observe the following behaviors: (a) period 1 process for $\omega = 2$, (b) period 2 process for $\omega = 3$, (c) period 3 process for $\omega = 3.45$, and (d) chaotic bouncing for $\omega = 4$, respectively.

translated to coordinates (u, v) at time moment t. This translation is sensitive to time t and coordinate x:

$$u = x + \eta(x, t),$$

$$v = \zeta(x, t),$$

$$(4.1)$$

where $\eta(x, t)$ and $\zeta(x, t)$ are predefined functions.

The condition that the particle is located on the surface leads to the following constraint:

$$v = \zeta(x, t), \qquad (4.2)$$
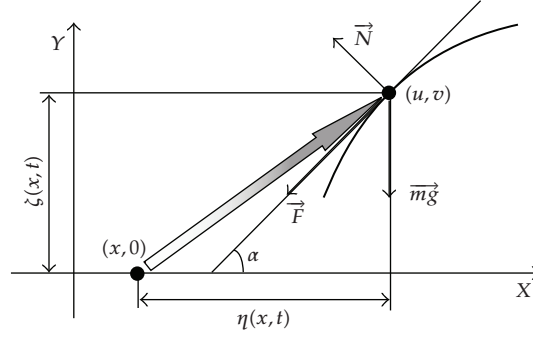
Figure 7: A geometric scheme of the dynamical system showing the particle sliding on the surface.

where x is to be found from the following algebraic equality (in which u is given and x is unknown):

$$x + \eta(x, t) = u. \tag{4.3}$$

Though the instantaneous shape of the oscillating surface cannot be described by an explicit function, the tangent to the surface at the point (u, v) can be expressed as

$$\tan \alpha = \frac{\zeta'_x(x, t)}{1 + \eta'_x(x, t)}. \tag{4.4}$$

Instantaneous velocities of the surface's point (u, v) in the direction of x- and y-axis can be expressed as follows:

$$\dot{u}|_{x=\text{const}} = \eta'_t(x, t),$$
$$\dot{v}|_{x=\text{const}} = \zeta'_t(x, t), \tag{4.5}$$

where dots denote derivatives by t.

When a mass particle slides on the surface, it does not necessarily move in contact with one point of the surface. Therefore x is no longer a constant. Thus,

$$\dot{u} = \dot{x}\left(1 + \eta'_x\right) + \eta'_t,$$
$$\ddot{u} = \ddot{x}\left(1 + \eta'_x\right) + \dot{x}^2\eta''_{xx} + 2\dot{x}\eta''_{xt} + \eta''_{tt}. \tag{4.6}$$

The condition that the mass particle continuously slides on the surface brings another constraint into force (the relative velocity in the normal direction to the surface at the contact point must be zero):

$$\tan \alpha = \frac{\dot{v} - \zeta'_t(x, t)}{\dot{u} - \eta'_t(x, t)}. \tag{4.7}$$

Equation (4.4) with (4.7) in force yields

$$\dot{v} = \frac{\dot{u} - \eta_t'}{1 + \eta_x'}\zeta_x' + \zeta_t',$$

(4.8)

which together with (4.6) produces the following relationship:

$$\dot{v} = \dot{x}\zeta_x' + \zeta_t'.$$

(4.9)

Differentiation of (4.9) yields

$$\ddot{v} = \ddot{x}\zeta_x' + \dot{x}^2\zeta_{xx}'' + 2\dot{x}\zeta_{xt}'' + \zeta_{tt}''.$$

(4.10)

Then the relative sliding velocity of the particle on the surface v_{12} can be expressed as

$$v_{12} = \left(\dot{u} - \eta_t'\right)\cos\alpha + \left(\dot{v} - \zeta_t'\right)\sin\alpha = \frac{\dot{x}}{\sqrt{1 + \tan^2\alpha}}\left(1 + \eta_x' + \zeta_x'\tan\alpha\right) = \dot{x}\sqrt{\left(1 + \eta_x'\right)^2 + \zeta_x'^2}.$$

(4.11)

The condition of dynamic equilibrium leads to the following system of equations:

$$m\ddot{u} + N\sin\alpha + F\cos\alpha = 0,$$
$$m\ddot{v} + mg + F\sin\alpha = N\cos\alpha,$$

(4.12)

where m is the mass of the particle; N is the reaction force at the contact point; g is the gravity acceleration; F is the friction force between the mass particle and the surface. The system of equations in (4.12) is in force when $N > 0$. Otherwise the particle jumps off the oscillating surface.

It is assumed that the friction force is linear. Thus F can be expressed like

$$F = hv_{12},$$

(4.13)

where h is the coefficient of linear friction.

Finally, the governing equation of motion can be derived from (4.12). Elementary transformations and substitutions lead to the following explicit differential equation:

$$B_1(x,t) \cdot \ddot{x} + B_2(x,t) \cdot \dot{x} + B_3(x,t) + B_4(x,t) \cdot (\dot{x})^2 = 0,$$

(4.14)

where

$$B_1(x,t) = m\left(1 + \eta'_x + \frac{(\zeta'_x)^2}{1 + \eta'_x}\right),$$

$$B_2(x,t) = 2m\left(\eta''_{xt} + \frac{\zeta'_x \zeta''_{xt}}{1 + \eta'_x}\right) + h\left(1 + \eta'_x + \frac{(\zeta'_x)^2}{1 + \eta'_x}\right),$$

$$B_3(x,t) = m\left(\eta''_{tt} + g\frac{\zeta'_x}{1 + \eta'_x} + \frac{\zeta'_x \zeta''_{tt}}{1 + \eta'_x}\right),$$

$$B_4(x,t) = m\left(\eta''_{xx} + \frac{\zeta'_x \zeta''_{xx}}{1 + \eta'_x}\right).$$

(4.15)

A major obstacle is eliminated, and direct numerical time marching techniques can be used for integration of (4.14)–computation of u and v is straightforward if the coordinate x is given at time t (4.1). Existence of a stability of the dynamic equilibrium can be analyzed explicitly.

But before proceeding with the analysis of dynamic equilibrium the following observation can be done. If kinematic relationships describing a traveling Rayleigh wave are in force, the change of variables

$$z = \omega t - kx \qquad (4.16)$$

transforms (4.14) to the following autonomous form:

$$C_1(z) \cdot \ddot{z} + C_2(z) \cdot \dot{z} + C_3(z) + C_4(z) \cdot (\dot{z})^2 = 0, \qquad (4.17)$$

where

$$C_1(z) = -\frac{m}{k}\left(1 - ka\cos(z) + \frac{k^2 b^2 \sin^2(z)}{1 - ka\cos(z)}\right),$$

$$C_2(z) = \frac{h}{m}C_1(z),$$

$$C_3(z) = \frac{\omega\, h}{k}\left(1 - ka\cos(z) + \frac{k^2 b^2 \sin^2(z)}{1 - ka\cos(z)}\right) + mg\frac{kb\sin(z)}{1 - ka\cos(z)},$$

$$C_4(z) = -m\left(a\sin(z) + \frac{kb^2 \sin(z)\cos(z)}{1 - ka\cos(z)}\right).$$

(4.18)

An important conclusion can be done. Dynamics of a particle sliding on the surface of a propagating Rayleigh wave cannot be chaotic. This is due to the fact that the governing equation of motion is a second-order autonomous ordinary differential equation with smooth parameter functions [30].

Equation (4.8) yields the dynamic equilibrium which represents a motion of the particle on a slope of the propagating wave with the velocity of its propagation:

$$\ddot{u} = 0,$$
$$\dot{u} = \frac{\omega}{k}, \tag{4.19}$$
$$u = \frac{\omega}{k} \cdot t - \psi,$$

where ψ is a constant. Then, it follows from (4.4) that

$$x + a\sin(\omega t - kx) = \frac{\omega}{k} \cdot t - \psi. \tag{4.20}$$

The term $a\sin(\omega t - kx)$ is bounded, therefore (4.20) will be in force when

$$x = \frac{\omega}{k} \cdot t - \theta, \tag{4.21}$$

where θ is a constant satisfying the equality $-\theta + a\sin(k\theta) = -\psi$. Moreover, conditions of existence of the dynamic equilibrium are similar in terms of x or u:

$$\dot{x} = \frac{\omega/k - \eta'_t}{1 + \eta'_x} = \frac{\omega}{k},$$
$$\ddot{x} = \frac{-\dot{x}^2\eta''_{xx} - 2\dot{x}\eta''_{xt} - \eta''_{tt}}{1 + \eta'_x} = 0. \tag{4.22}$$

As mentioned earlier, the explicit governing equation is formulated in terms of x, not the coordinate of the contact point u. First, coordinates of the unstable saddle point are determined. Then coordinates of the same saddle point are calculated in the frame $(\omega t - ku)$; $\dot{u}$ using the relationship in (4.3). Forward and reverse time marching techniques are used to construct basin boundaries of attractors when partial solutions of (4.14) are sought from the infinitesimal surrounding of the saddle point.

The described computational technique is used to construct basin boundaries of the system's attractors (Figure 8). Solutions in terms of u (forward and reverse) are visualized only. It can be noted that two stable attractors can coexist–a stable equilibrium point and a stable limit cycle. Shaded regions in Figure 8 correspond to a basin (attracting set of initial conditions) of stable equilibrium points, while white region corresponds to a basin of the limit cycle. The phase plane in Figure 8 is periodic by 2π and can be visualized in cylindrical coordinates, but the plane representation is clearer.

A special attention should be paid to dashed line intervals on basin boundaries. Equation (4.14) describes a motion of a particle on the surface of a propagating wave. This governing equation of motion holds until the reaction force N in (4.12) is positive. Whenever N gets equal or lower than zero, the particle looses a contact with the surface and starts a free fly in a gravitational field until it bounces on the surface again. Therefore, the moment when the particle looses the contact with, the surface is detected, and the trajectory is marked by
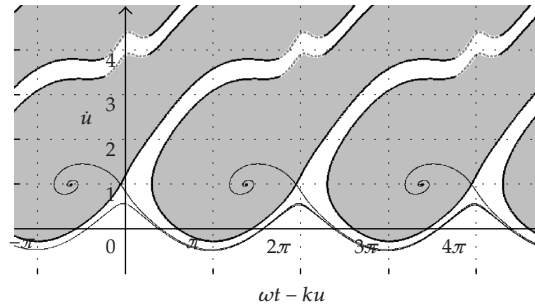
Figure 8: Basin boundaries at $b = 0.5$; $a = b = 1.5$; $m = 0.4$; $h = 0.1$; $\omega = k = 1$, shaded regions illustrate the basin of attraction of stable equilibrium points.
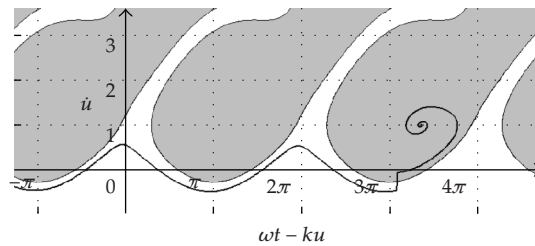
Figure 9: Illustration of the attractor control strategy: limit cycle is represented as a periodic trajectory in frame $(\omega t - ku; \dot{u})$; small external impulse kicks the trajectory to basin boundary of stable equilibrium point where the particle eventually settles down.

a dashed line. It can be noted that such motions occur only at relatively high particle velocities (Figure 8).

Conveyance of a particle by a propagating Rayleigh wave is a nonlinear problem, so such effects as the coexistence of stable attractors should not be astonishing. Stable equilibrium point type attractor in Figure 8 corresponds to a surf-type motion on a slope of a propagating wave; stable limit cycle corresponds to a motion with an average velocity much lower than the velocity of the propagating wave. Coexistence of attractors (a stable equilibrium point and a stable limit cycle) enables development of motion control strategies based on a small external impulses which can bring the system from the regime of motion with small average velocity into motion with the propagating wave's velocity [21]. Such attractor control strategy is illustrated in Figure 9 where the particle first oscillates in the limit cycle, and then a small external impulse kicks it to the basin of attraction of the stable focus point.

It can be noted that the up-mentioned control strategy can be implemented only when the stable equilibrium point and the stable limit cycle coexist. Thus, it would be impossible to transport a sand particle with the velocity of the propagating wave by an acoustic surface Rayleigh wave. Nevertheless, such attractor control strategies could be implemented for transportation of biomedical objects on the surface of an undulation film [21]. The sliding particle model presented in this section also exhibits a very rich dynamics as in the case of the bouncer model. In particular, the sliding particle model should also have the sensitivity to the initial conditions for certain sets of parameter values as occuring in the bouncer model

(see [22]). The sensitivity of transient processes to initial conditions takes place for both, the bouncer model and the sliding particle model.

5. Conclusions and Discussion

Transport of particles by surface waves is an important scientific and engineering problem, with numerous practical applications, including MEMS (micro-electro-mechanical systems) used to manipulate objects like particles or cells. We show that this problem is a modification of the classical bouncer model which is considered as a paradigm model in nonlinear physics. The formulations of our model are implicit, thus phase and velocity maps cannot be expressed in explicit form.

Chaotic dynamics of a conveyed particle is not an unexpected fact due to the complexity of the constitutive model. More surprising is the rich dynamical behavior in models comprising dissipative dynamics, elastic and inelastic collisions. It appears that the transition to chaos via a period doubling route is a universal property for bouncers and is observed in our model of particles transport in both, conservative and viscous media. Moreover, the sensitivity to initial conditions can be useful for control techniques which can dramatically increase the effectiveness of particles transport by surface waves. These results are relevant in the sense that we have also found the sensitivity to the initial conditions for the sliding particle model, which may have important applications in practical implementations as powder transport by piezoelectrically excited ultrasonic waves, transport of sand particles, among others.

Though the numerical analysis was concentrated on the dimensionless system only, theoretical and experimental investigation of dry particle conveyance and its control is a definite object for future research.

Acknowledgments

References

[1] G. M. Zaslavsky, "The simplest case of a strange attractor," *Physics Letters A*, vol. 69, no. 3, pp. 145–147, 1978.

[2] L. D. Pustilnikov, "On Ulam's problem," *Theoretical and Mathematical Physics*, vol. 57, p. 1035, 1983.

[3] M. A. Lieberman and A. J. Lichtenberg, "Stochastic and adiabatic behavior of particles accelerated by periodic forces," *Physical Review A*, vol. 5, no. 4, pp. 1852–1866, 1972.

[4] E. Fermi, "On the origin of the cosmic radiation," *Physical Review*, vol. 75, no. 8, pp. 1169–1174, 1949.

[5] B. V. Chirikov, "A universal instability of many-dimensional oscillator systems," *Physics Reports*, vol. 52, no. 5, pp. 264–379, 1979.

[6] A. J. Lichtenberg, M. A. Lieberman, and R. H. Cohen, "Fermi acceleration revisited," *Physica D*, vol. 1, no. 3, pp. 291–305, 1980.

[7] P. Pieranski and J. Malecki, "Noisy precursors and resonant properties of the period-doubling modes in a nonlinear dynamical system," *Physical Review A*, vol. 34, no. 1, pp. 582–590, 1986.

[8] R. M. Everson, "Chaotic dynamics of a bouncing ball," *Physica D*, vol. 19, no. 3, pp. 355–383, 1986.

[9] K. Wiesenfeld and N. B. Tufillaro, "Suppression of period doubling in the dynamics of a bouncing ball," *Physica D*, vol. 26, no. 1–3, pp. 321–335, 1987.

[10] Z. J. Kowalik, M. Franaszek, and P. Pierański, "Self-reanimating chaos in the bouncing-ball system," *Physical Review A*, vol. 37, no. 10, pp. 4016–4022, 1988.

[11] M.-O. Hongler, P. Cartier, and P. Flury, "Numerical study of a model of vibro-transporter," *Physics Letters A*, vol. 135, no. 2, pp. 106–112, 1989.

[12] M.-O. Hongler and J. Figour, "Periodic versus chaotic dynamics in vibratory feeders," *Helvetica Physica Acta*, vol. 62, no. 1, pp. 68–81, 1989.

[13] M. Mracek and J. Wallaschek, "A system for powder transport based on piezoelectrically excited ultrasonic progressive waves," *Materials Chemistry and Physics*, vol. 90, no. 2-3, pp. 378–380, 2005.

[14] M. S. Talary, J. P. H. Burt, J. A. Tame, and R. Pethig, "Electromanipulation and separation of cells using travelling electric fields," *Journal of Physics D*, vol. 29, no. 8, pp. 2198–2203, 1996.

[15] C.-F. Chou, J. O. Tegenfeldt, O. Bakajin, et al., "Electrodeless dielectrophoresis of single- and double-stranded DNA," *Biophysical Journal*, vol. 83, no. 4, pp. 2170–2179, 2002.

[16] R. H. Plaut, A. L. Farmer, and M. M. Holland, "Bouncing-ball model of 'dry' motions of a tethered buoy," *Journal of Vibration and Acoustics*, vol. 123, no. 3, pp. 333–339, 2001.

[17] J. D. Achenbach, *Wave Propagation in Elastic Solids*, Elsevier, New York, NY, USA, 1984.

[18] L. D. Landau and E. M. Lifshitz, *Theory of Elasticity*, Pergamon Press, Oxford, UK, 1986.

[19] K. Aki and P. G. Richards, *Quantitative Seismology*, Freeman, New York, NY, USA, 1980.

[20] C. M. Flannery and H. Von Kiedrowski, "Dispersion of surface acoustic waves on rough anisotropic materials," in *Proceedings of the IEEE Ultrasonics Symposium*, vol. 1, pp. 583–586, 2001.

[21] M. Ragulskis and K. Koizumi, "Applicability of attractor control techniques for a particle conveyed by a propagating wave," *Journal of Vibration and Control*, vol. 10, no. 7, pp. 1057–1070, 2004.

[22] M. Ragulskis and M. A. F. Sanjuán, "Transport of particles by surface waves: a modification of the classical bouncer model," *New Journal of Physics*, vol. 10, Article ID 083017, 2008.

[23] J. M. Luck and A. Mehta, "Bouncing ball with a finite restitution: chattering, locking, and chaos," *Physical Review E*, vol. 48, no. 5, pp. 3988–3997, 1993.

[24] R. M. May, "Simple mathematical models with very complicated dynamics," *Nature*, vol. 261, no. 5560, pp. 459–467, 1976.

[25] C.-F. Chou, J. O. Tegenfeldt, O. Bakajin, et al., "Electrodeless dielectrophoresis of single- and double-stranded DNA," *Biophysical Journal*, vol. 83, no. 4, pp. 2170–2179, 2002.

[26] L. Cui and H. Morgan, "Design and fabrication of travelling wave dielectrophoresis structures," *Journal of Micromechanics and Microengineering*, vol. 10, no. 1, pp. 72–79, 2000.

[27] A. D. Dussaud, B. Khusid, and A. Acrivos, "Particle segregation in suspensions subject to high-gradient ac electric fields," *Journal of Applied Physics*, vol. 88, no. 9, pp. 5463–5473, 2000.

[28] W. N. Hassan and J. S. Ribberink, "Transport processes of uniform and mixed sands in oscillatory sheet flow," *Coastal Engineering*, vol. 52, no. 9, pp. 745–770, 2005.

[29] S. D. Wang, Y. M. Shen, and Y. H. Zheng, "Two-dimensional numerical simulation for transport and fate of oil spills in seas," *Ocean Engineering*, vol. 32, no. 13, pp. 1556–1571, 2005.

[30] R. C. Hilborn, *Chaos and Nonlinear Dynamics*, Oxford University Press, New York, NY, USA, 1994.